ACS APPLIED BIO MATERIALS

www.acsabm.org Article

Biochar-Supported Cu^{2+}/Cu^{+} Composite as an Electrochemical Ultrasensitive Interface for Ractopamine Detection

Liping Cao, Qi Ding, Minghuan Liu, Hetong Lin,* and Da-Peng Yang*

Cite This: *ACS Appl. Bio Mater.* 2021, 4, 1424−1431 Read Online

ACCESS | Metrics & More | Article Recommendations | Supporting Information

ABSTRACT: Ractopamine as an important β-agonist is frequently found in pork to enhance food quality, which is harmful to human health. Thus, it is extremely important to develop an efficient analytical method to detect ractopamine for food safety control. Herein, we develop a kind of electrochemical biosensor using a biochar-supported Cu^{2+}/Cu^{+} composite as an electrochemical sensing interface for detecting ractopamine. The electrochemical sensor combines the collective advantages of Nafion (enriches ractopamine and effectively shields the interference of negatively charged compounds), biochar (unique three-dimensional porous network structure to increase the contact area), and Cu^{2+}/Cu^{+} (excellent electrical conductivity to speed up the charge transfer rate), which are beneficial to the accumulation and electrochemical sensing of targets on a Nafion-biochar-supported Cu^{2+}/Cu^{+} electrode (NBC-GCE). The as-prepared sensor shows a good electrochemical sensing ability, with an ultralow detection limit and high sensitivity (0.041 μM and 416 $\mu A \cdot mM^{-1} \cdot cm^{-2}$, respectively), in the 0.1−1.75 μM range. In addition, the stability, repeatability, and anti-interference performance of the modified electrode are also satisfying. Last, its practicability is shown for assaying ractopamine in pork sausages. This research provides an environmentally friendly method to simultaneously treat food waste and achieve ultrasensitive detection of ractopamine in food.

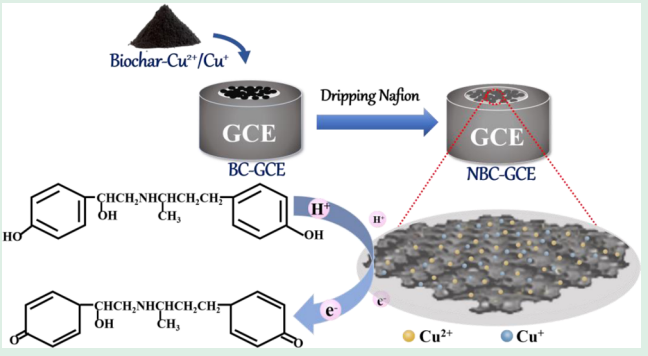

KEYWORDS: *ractopamine, eggshell membrane, Cu^{2+}/Cu^{+} redox couple, food detection, electrochemical sensors*

1. INTRODUCTION

Ractopamine, an important β-agonist, is often found in pork as a residual contaminant that is harmful to human health.[1] In the 1980s, some researchers discovered that ractopamine could increase the lean rate of animals, so it was illegally used in animal breeding.[2,3] Since ractopamine remains in animals for a long time and has certain toxicity, ingestion of meat products containing ractopamine may pose a certain threat to human health.[4−6] Therefore, research and development of technologies and methods for detecting ractopamine in meat products are of significance for maintaining food safety and human health.[7,8]

So far, some different analytical methods have been developed to detect ractopamine. These methods mainly include high-performance liquid chromatography (HPLC),[9] gas and liquid chromatography (GC and LC, respectively) GC−MS,[10] LC−MS,[11] capillary electrophoresis,[12] and immunoassay.[13] Compared with the above analysis methods, the electrochemical detection of ractopamine has the advantages of low cost, less time-consuming, simple instrument operation, high sensitivity, and so on.[14] At present, many researchers have made great progress in this area. But ordinary electrodes have a low response to ractopamine and poor detection signals, so it is necessary to modify the electrodes. Although the performance of the modified electrode had been improved, the sensitivity and selectivity of electrode detection should still be greatly improved. Therefore, developing novel technologies and methods for detecting ractopamine in meat products is of great importance for maintaining food safety and human health.

Eggs are a kind of high-quality and inexpensive animal protein food and one of the most economical sources of animal protein. It is an important part of the diet of urban and rural residents.[15] Affected by traditional consumption habits, the consumption of eggs of Chinese residents is mainly composed of fresh eggs. Therefore, a large amount of eggshell garbage is generated every year, which puts huge pressure on urban garbage disposal and environment.[16,17] The eggshell membrane (ESM) is in between the egg white and the shell, which is rich in proteins and fiber.[18] It is widely used to adsorb metal ions in water. For example, in previous work, we used an

Received: October 9, 2020
Accepted: January 12, 2021
Published: January 21, 2021

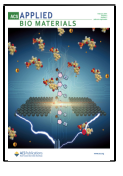

https://dx.doi.org/10.1021/acsabm.0c01314
ACS Appl. Bio Mater. 2021, 4, 1424−1431

eggshell membrane to adsorb Cu^{2+} and Zn^{2+} and obtained CuO/ZnO-ESM nanocomposites after the water treatment.[19] In another work, we used the eggshell membrane and Au^{3+} to prepare AuNP/ESM nanocomposites capable of detecting pesticide residues in oolong tea.[20] Zhang et al. deposited gold nanoparticles on the three-dimensional porous carbonized eggshell membrane and fabricated a sensitive and noble ampere horseradish peroxidase biosensor.[21] These studies showed that ESM is an excellent material and is worthy of our continued exploration.

Metal nanomaterials are considered to be "star products" in chemically modified electrodes due to their many excellent properties.[22] At present, great progress has been made in the field of electrochemical sensing using metal nanomaterials. Compared with the noble metal nanomaterials, copper (Cu) has the advantages of low cost, high catalysis, strong conductivity, and antibacterial properties.[23] However, the storage activity is very low due to its easy oxidation at room temperature. To solve this problem, fabricating Cu^{2+}/Cu^{+} redox couples might become a smart strategy.[24] This is because many experiments have proved that the Cu^{2+}/Cu^{+} redox couple has similar properties to Cu nanomaterials, but it is more stable than the latter.[25] To make the Cu^{2+}/Cu^{+} redox couple fully play its role on the electrode surface, carbon-based materials (i.e., activated carbon, graphene oxide, and carbon nanotubes) are often used as support materials.[26] In this work, the calcined ESM was used as the support material of the Cu^{2+}/Cu^{+} redox couple. Its high surface area and hierarchical porous architecture provide more reaction sites for the Cu^{2+}/Cu^{+} redox couple, which helps the subsequent electrochemical catalysis system. Nafion, a perfluorinated sulfonated cation exchanger with high chemical and thermal stability and mechanical strength, is also often used as a cation exchange membrane.[27] Moreover, since Nafion is negatively charged, it can suppress interference caused by negatively charged impurities.[28] In previous studies, it has been demonstrated that Nafion-modified electrodes can be used to detect organic compounds and metal cations well.[29,30]

In this study, the ESM was used to absorb Cu^{2+} ions in an aqueous solution and calcined to form a biochar-Cu^{2+}/Cu^{+} composite (abbreviated as BC) in air. It was then adsorbed on the glass carbon electrode (GCE) surface and combined with Nafion to fabricate a novel sensing interface Nafion-biochar-Cu^{2+}/Cu^{+} (abbreviated as NBC). Such prepared sensing interface not only has the extremely large specific surface area and synergistic catalytic performance exerted by biochar and the Cu^{2+}/Cu^{+} redox couple but also has the effect of enriching targets due to the charge interaction between Nafion and ractopamine. As a result, it was found that the composite could increase the protonation degree of the electrochemical group (hydroxyl) of ractopamine, with a larger electrode current and higher sensitivity. In addition, the analytical performance of the electrochemical sensor was evaluated by measuring ractopamine in sausages.

2. EXPERIMENTAL SECTION

2.1. Reagents. Ractopamine hydrochloride ($C_{18}H_{22}NO_3$·HCl, Rac) was obtained from Manhag Biotechnology Co. (Beijing, China). Nafion was purchased from Alfa Aesar Chemical Co. $CuCl_2$ was ordered from Sinopharm Chemical Reagent Co. (China). NaH_2PO_4 and Na_2HPO_4 were bought from Maclean Biotechnology Co. (China). Glucose (Glu), uric acid (UA), glycine (Gly), ascorbic acid (AA), and dopamine (DA) were purchased from Xilong Chemical Co. All initial materials were of analytical grade. The eggshell membrane was from the faculty dining room.

2.2. Apparatus. The morphologies of the biochar-Cu^{2+}/Cu^{+} composites were analyzed using a Zeiss field emission scanning electron microscope (FESEM) coupled with X-ray energy dispersive spectroscopy (EDS). The X-ray diffraction (XRD) spectrum of the sample was obtained by a Bruker (D8 Advanced) X-ray diffractometer. The Raman spectra were recorded using an instrument manufactured by Renishaw Via (U.K.). X-ray photoelectron spectroscopy (XPS) was performed using a Kratos Axis Ultra DLD instrument. The electrochemical experiments were carried out using a CHI660E setup containing the working, reference, and counter electrodes (GCE, Ag/AgCl/KCl, and Pt-wire, respectively).

2.3. Material Synthesis. The synthesis of the biochar-Cu^{2+}/Cu^{+} composite was carried out following the method reported elsewhere.[31] Briefly, we peeled the ESM from the eggshell with tweezers, and then washed it with hydrochloric acid and water several times and dried it. The dried ESM was ground into a powder and stored for later use. One gram of the ESM powder was mixed with 50 mL of a 0.01 M $CuCl_2$ solution and allowed to react for 24 h, after which 50 mL of 0.01 M VC was added. After another 24 h, the mixture was filtered, rinsed, dried, and calcined at 250 °C for 2 h. The resulting material was a biochar-Cu^{2+}/Cu^{+} composite (BC).

2.4. Preparation of NBC-GCE. First, we polished the electrode and prepared a 2 mg mL^{-1} biochar-Cu^{2+}/Cu^{+} dispersion. Second, 6 μL of the CB suspension was dropped onto the electrode and allowed to dry naturally. Finally, 6 μL of Nafion was dropped on the CB-GCE surface and dried to obtain the Nafion-biochar-Cu^{2+}/Cu^{+}-GCE (NCB-GCE).

2.5. Sample Preparation. The pork sausage sample was crushed at first, and 2.0 g of the crushed sample was taken out, 4 mL (0.1 M) of $HClO_4$ was added to it, and then ultrasonicated for 30 min. The above materials were reacted in water at 80 °C for 30 min. A supernatant was collected by centrifuging the cooled (to ambient temperature) mixture at 10 000 rpm for 15 min. The pH of the collected supernatant was adjusted to 10 using 10% Na_2CO_3. NaCl (1.5 g) was also added. The solution was extracted with 5 mL of ethyl acetate, and then Rac was back-extracted into a HCl solution, and the operation was repeated several times. Finally, the solution was diluted to 10 mL with pH 7 phosphate-buffered saline (PBS).

3. RESULTS AND DISCUSSION

3.1. Characterization Results. Scanning electron microscopy (SEM) analysis confirmed that the natural ESM was composed of protein and an interwoven three-dimensional network (see Figure 1A). These intertwined networks mainly contain collagen and glycoproteins and look very smooth, revealing the inherent and dense structure of the inner surface of the original ESM. The surface morphology of biochar-Cu^{2+}/Cu^{+} (Figure 1B,C) is similar to that of the natural ESM, but its subtle surface texture is not as smooth as the natural ESM, which also provides more contact area for Cu^{2+}/Cu^{+}. At the same time, we also did the Brunauer–Emmett–Teller (BET) analysis of both biochar-Cu^{2+}/Cu^{+} and the natural ESM and compared the surface areas, pore volumes, and sizes of the two materials (see Figure S1 and Table S1). The EDS element mapping image further illustrates the element composition and distribution of biochar-Cu^{2+}/Cu^{+}, confirming the existence and uniform distribution of Cu, C, N, and O elements (see Figure 1D).

The molecular structures of both the natural ESM and biochar-Cu^{2+}/Cu^{+} were characterized spectroscopically. Fourier transform infrared (FTIR) of the ESM (Figure 2A(b)) revealed a broad peak at 3461 cm^{-1}, which corresponded to the stretching vibrations of N–H and O–H groups. The peaks at 1715 and 1653 cm^{-1} corresponded to the stretching of C–O and C═O groups, respectively. A band at 1521 cm^{-1} was

https://dx.doi.org/10.1021/acsabm.0c01314
ACS Appl. Bio Mater. 2021, 4, 1424–1431

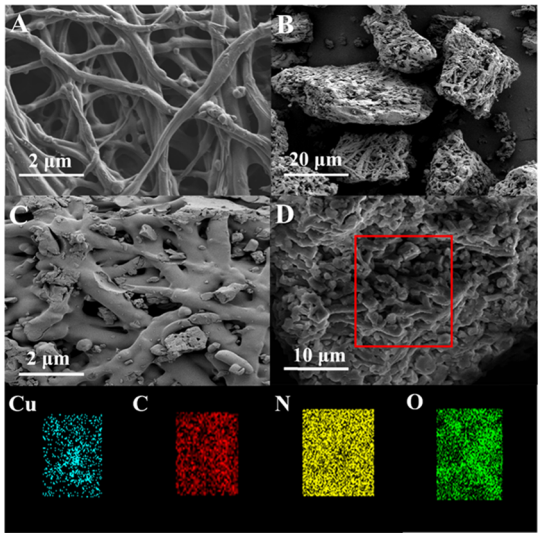

Figure 1. FESEM micrographs of (A) ESM and (B, C) biochar-Cu^{2+}/Cu^{+}. (D) Elemental mapping obtained by EDS for the biochar-Cu^{2+}/Cu^{+} composite.

ascribed to the tensile vibration of the C−N−H group. The peaks at 1395 and 1189 cm^{-1} belonged to C−O stretching vibrations.

FTIR of the composite material showed two broad peaks at 3462 and 1373 cm^{-1} (see Figure 2A(a)), belonging to the stretching of O−H and C−O bonds, respectively. The peak at 1611 cm^{-1} belonged to the C═O vibration.[32] The Raman spectrum of the biochar-Cu^{2+}/Cu^{+} composite showed the D and G bands (see Figure 2B), which were similar to those observed for graphene.[33] Thus, the composite has a similar structure to graphene.

The composition and metal valence of biochar-Cu^{2+}/Cu^{+} composites have been systematically studied by XPS. The XPS spectrum of biochar-Cu^{2+}/Cu^{+} showed four peaks at 932, 284.5, 399.7, and 531.5 eV, belonging Cu 2p, C 1s, N 1s, and O 1s, respectively. Cu $2p_{1/2}$ and Cu $2p_{3/2}$ peaks were at 954.4 and 934.5 eV (see Figure 3A) and corresponded to Cu^{2+} and Cu^{+}, respectively. A peak at 943.1 eV further confirmed the presence of Cu^{2+} because the oscillation peak would not appear without the Cu^{2+} species.[34] Peaks corresponding to C−C and C═O positioned at 284.7 and 287.9 eV were also detected (see Figure 3B), while the N 1s peak was visible at 400.0 eV and attributed to N−C (Figure 3C). The O 1s spectrum showed one peak at 532.5 eV; the BC nanocomposite has only one peak corresponding to C═O (Figure 3D).[35]

3.2. Electrochemical Performance of the NBC-GCE Modified Electrode. The surface conductivity of our electrodes was assessed using electrochemical impedance spectroscopy (EIS). Our EIS spectra were typical and contained semicircular and linear parts. As shown in Figure 4A, the Randles circuit is used to fit the acquired impedance data. In Figure 4A, we can see that the redox reactions of $[Fe(CN)_6]^{3-/4-}$ on the bare GCE (curve a) exhibited a larger semicircle. In addition, the EIS diagram of the BC-GCE is presented in Figure S2. The semicircle diameter of the NBC-GCE (curve b) is somewhere in between, which indicates that Nafion can exist as an inert layer and prevent the diffusion of ferricyanide on the electrode. Our cyclic voltammetry (CV) results (shown in Figure S3) confirmed these conclusions.

Next, we used CV to prove that the NBC-modified electrode could detect ractopamine in the mixed solution. The current change was measured at a scan rate of 100 $mV{\cdot}s^{-1}$ in 0.2 M PBS with pH = 7.0. The CV curve of 2.0×10^{-6} M ractopamine on the bare GCE (curve c) did not show any obvious redox peaks (see Figure 4B). The CV data (curve d) of ractopamine on the NBC-GCE only showed a small oxidation peak near −0.29 V, while the corresponding reduction peak was not observed in the reverse scan. The results showed that ractopamine was irreversible on the NBC-GCE. Curves a and b showed that when there was no ractopamine in the solution, the bare GCE and the NBC-GCE did not show corresponding oxidation peaks. By modifying the BC on the GCE, the contact area could be improved, and the detection efficiency of the electrode could also be enhanced. In addition, the Nafion membrane is negatively charged and easily adsorbs the positively charged ractopamine in the solution, which can enrich the analyte in electrochemical detection. This enrichment demonstrated an excellent selectivity to ractopamine. The sensitivity of ractopamine detection was also improved. Therefore, we believe that the presence of NBC-modified GCE is advantageous for ractopamine oxidation.

3.3. Effect of pH on the Oxidation of Ractopamine on the NBC-GCE. The solution pH affects ractopamine oxidation on the NBC-GCE. The effects of different pH values (5.5−8.0) on the oxidation of ractopamine in the presence of 2.0×10^{-6} M ractopamine in 0.2 M PBS were studied by CV (Figure 5A). The peak current increased as the pH was increased from 5.5 to 7.0 (see Figure 5B). However, as the pH was increased to 8.0, the peak current decreased. Therefore, pH = 7.0 was chosen for all further tests. Simultaneously, the anode peak potential of ractopamine shifted negatively as the pH was increased because of the deprotonation effect that promotes the oxidation of Rac at higher pH values. In addition, the change in peak potential with pH follows the linear equation

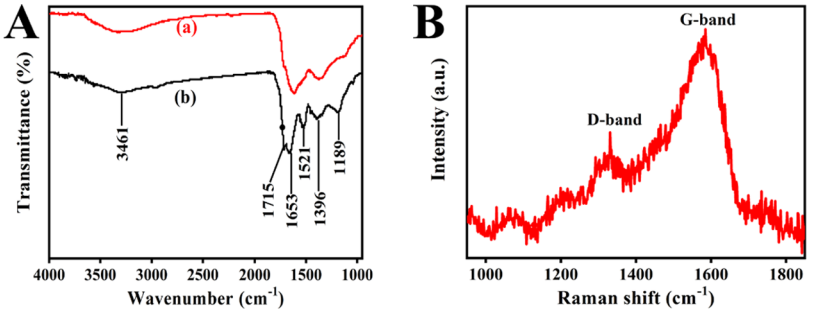

Figure 2. (A) FTIR spectrum of the ESM (b) and the biochar-Cu^{2+}/Cu^{+} composite (a). (B) Raman spectrum of the biochar-Cu^{2+}/Cu^{+} material.

https://dx.doi.org/10.1021/acsabm.0c01314
ACS Appl. Bio Mater. 2021, 4, 1424−1431

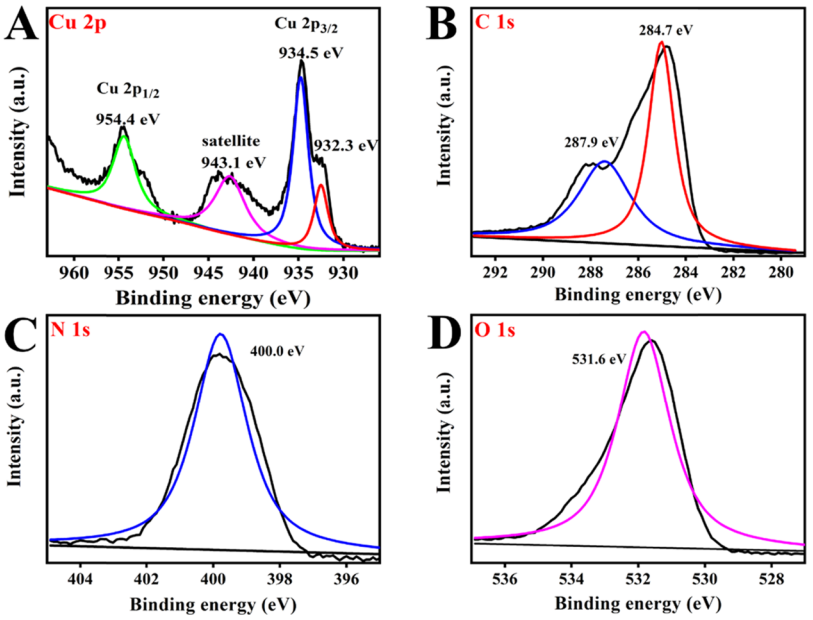

Figure 3. (A) Cu, (B) C, (C) N, and (D) O XPS spectra for the BC composites prepared in this work.

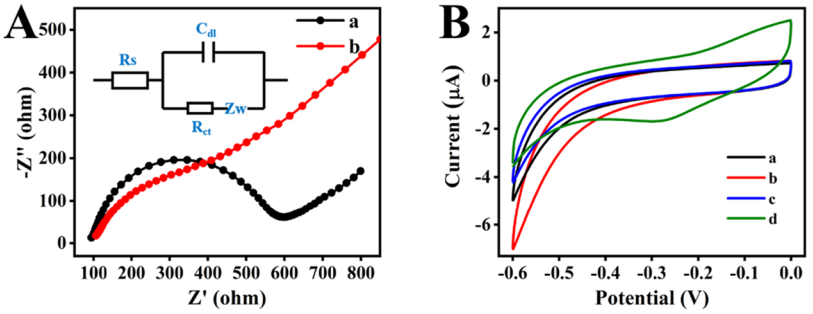

Figure 4. (A) EIS of the GCE (a) and the NBC-GCE (b). (B) CV spectra of the bare GCE and the NBC-GCE without (a, b) and with (c, d) of 2.0×10^{-6} M ractopamine. Spectra were recorded at 100 mV·s^{-1} using PBS with pH = 7.

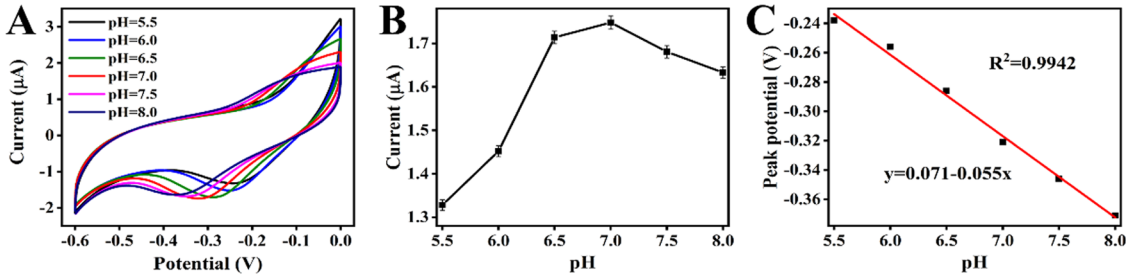

Figure 5. (A) CV spectra (on the NBC-GCE surface) collected at a scan rate of 100 mV·s^{-1}. (B) Peak current and (C) peak potential of 2.0×10^{-6} M ractopamine as a function of pH.

E_{pa} = 0.071−0.055 pH (R^2 = 0.9942) (Figure 5C). The slope of the equation (−55 mV/pH) was close to the theoretical value (−59 mV/pH). Therefore, the number of protons transferred during the ractopamine oxidation on the NBC-GCE surface was equal to the number of electrons.

3.4. Scan Rate Effect on the Ractopamine Oxidation on the NBC-GCE Surface. At the same time, we studied how the scanning rate affected the ractopamine oxidation peak current and used the obtained data to explain the oxidation mechanism on the NBC-GCE surface. The CV tests were performed using 2.0×10^{-6} M ractopamine dissolved in 0.2 M PBS with pH = 7.0 (see Figure 6A). The oxidation peak current was linearly dependent on the scan rate (see Figure 6B) and was fitted by the equation I_{pa} = 1.302 + 0.0075ν (R^2 = 0.9993). Thus, ractopamine oxidation on the NBC-GCE surface was an adsorption-controlled process. Laviron's theory[36] defines the E_{pa}/lg ν relationship as follows

$$E_{pa} = E^{0\prime} + (2.303RT/\alpha n_a F)\lg(RTk^0/\alpha n_a F) + (2.303RT/\alpha n_a F)\lg\nu \quad (1)$$

From Figure 6C, we can see that the linear relationship between the values of E_{pa} and lg ν in this experiment is as follows2

https://dx.doi.org/10.1021/acsabm.0c01314
ACS Appl. Bio Mater. 2021, 4, 1424−1431

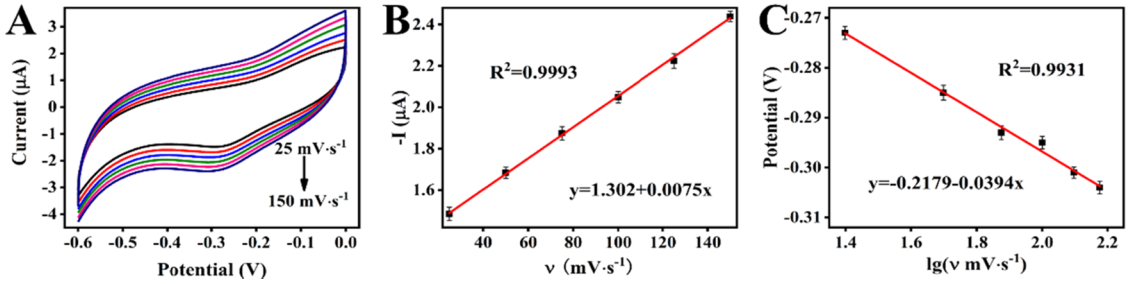

Figure 6. (A) CV curves for 2.0×10^{-6} M ractopamine oxidation on the NBC-GCE surface recorded at 25−150 mV·s^{-1} rates in PBS with pH = 7.0. Scan rate as a function of the peak current (B) and its logarithm (C) and the corresponding fitting curves (red straight lines).

$$-E_{pa} = 0.2179 + 0.0394 \lg \nu, \ (R^2 = 0.9930) \quad (2)$$

The value of αn calculated by combining eqs 1 and 2 was equal to 0.7742. The n_a value of completely irreversible electrode processes is typically in the 0.4−0.6 range. By calculation, the value of n_a is approximately equal to 2. Thus, the ractopamine oxidation reaction on the NBC-GCE surface involved one pair of protons and one pair of electrons (see Scheme 1).

Scheme 1. Ractopamine Oxidation Mechanism on the NBC-GCE Surface

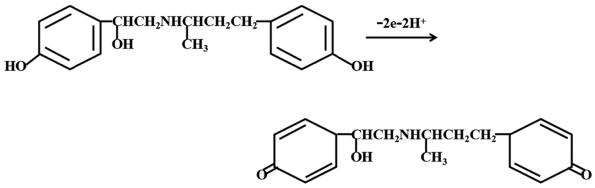

3.5. Ractopamine Detection as a Function of Its Suspension Volume, Accumulation Potential, and Detection Time.

The ractopamine peak current changed with the volume of the NBC suspension according to the differential pulse voltammetry (DPV) tests (see Figure 7A). It was found that when the amount of the suspension was 0−6 μL, the peak current of ractopamine increased significantly. This is because NBC can increase the effective area of the GCE surface, thereby enhancing the cumulative efficiency and peak current. When the volume of the NBC suspension was increased from 6 to 10 μL, the peak current increased insignificantly, indicating that the NBC was saturated on the GCE surface. Due to comprehensive considerations, we use 6 μL of the NBC suspension to modify the electrode surface.

The ractopamine oxidation peak currents accumulated at −0.9 to −0.4 V for 3 min were measured to understand the effect of the accumulated potential (see Figure 7B). The results showed that when the cumulative potential changed from −0.9 to −0.6 V, the oxidation peak current slightly increased. At −0.4 V, the peak value of ractopamine oxidation decreased significantly. Therefore, the −0.6 V accumulation potential was used for all further tests. All DPV scans were recorded starting from −0.6 V.

We also examined how the accumulation time affected the peak current of ractopamine oxidation (see Figure 7C). The results showed that as the accumulation time increased from 0 to 3 min, the peak oxidation current also increased. Thus, the accumulation approach is an effective method to enhance sensitivity. At an accumulation time of 5 min, the ractopamine oxidation peak current increased slightly because the ractopamine content on the NBC surface was approaching its limit. Considering the detection sensitivity and analysis speed, an accumulation time of 3 min is used.

3.6. Linear Range, Repeatability, and Stability of Ractopamine Detection.

Differential pulse voltammetry (DPV) can register changes occurring during reactions with low ractopamine concentrations. Therefore, we used the DPV method to study the electrocatalytic behavior of ractopamine (Figure 8A). The ractopamine concentration on the NBC-GCE increased from 0.1 to 1.75 μM, and its peak current linearly increased (see Figure 8B) following the $I_{pa} = 1.733 + 0.146C$ equation with the correlation coefficient $R^2 = 0.997$.

The electrode detection limit (LOD) is calculated according to the following formula

$$\mathrm{LOD} = 3\delta/k$$

where δ is the relative standard deviation of the NBC-GCE electrode measured 5 times in PBS solution, which was equal to 0.041 μM. The sensitivity was 416 μA·mM^{-1}·cm^{-2}. Thus, the sensitivity and LOD of the NBC-GCE were significantly better than ractopamine electrochemical sensors reported in the literature (Table 1).

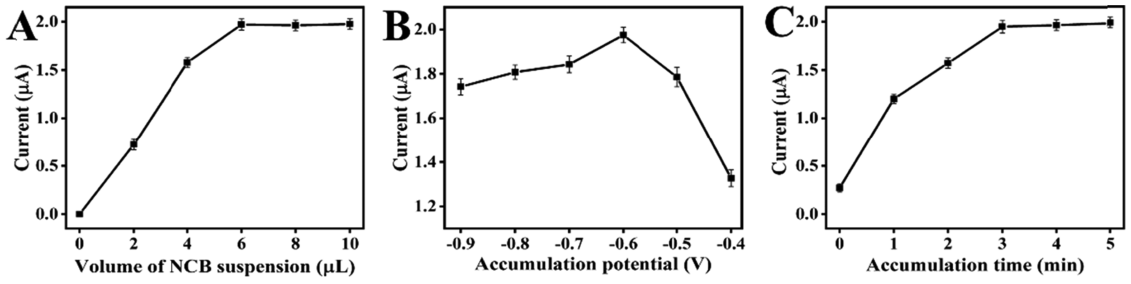

Figure 7. Influence of NBC suspension volume (A), accumulation potential (B), and time (C) on the oxidation peak current of 2.0×10^{-6} M ractopamine. Measurements were performed at a scan rate of 100 mV·s^{-1} in 0.2 M PBS with pH = 7.0.

https://dx.doi.org/10.1021/acsabm.0c01314
ACS Appl. Bio Mater. 2021, 4, 1424−1431

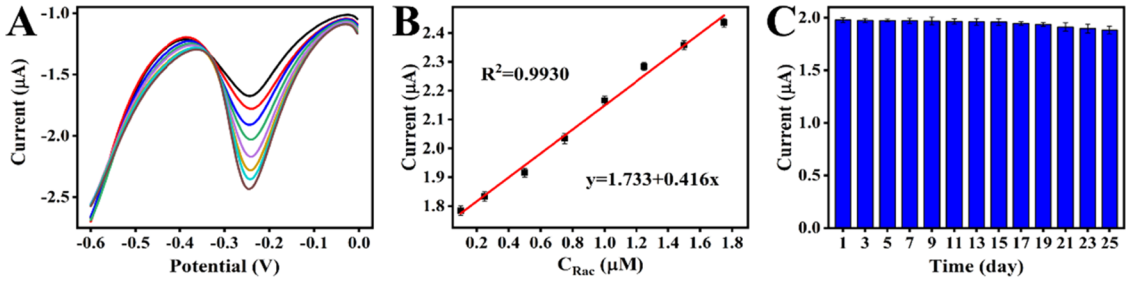

Figure 8. (A) DPV curves at different ractopamine concentrations at the NBC-GCE surface. (B) Calibration curve of ractopamine concentration and peak current. (C) Stability of NBC-modified GCE after tests for 25 consecutive days.

Table 1. Linear Ranges and LOD of Different Modified Electrodes Fused for Ractopamine Detection

electrodes	linear range (μM)	LOD (μM)	ref
PCit/GCE[a]	0.14−5.41	0.001	37
G/GNR/GCE[b]	0.001−2.7	0.00051	38
OMC/GCE[c]	0.085−8.0	0.06	39
GO/GCE[d]	0.074−2.96	0.056	40
NBC/GCE	0.1−1.75	0.041	this work

[a]Polycitrulline-modified GCE. [b]Graphene/gold nanorod-modified GCE. [c]Ordered mesoporous carbon-modified GCE. [d]GO-modified GCE.

We prepared five different modified electrodes using identical conditions to detect 2.0×10^{-6} M ractopamine. The relative standard deviation (RDS) is equal to 3.3%, indicating that the NBC-GCE has good repeatability in detecting ractopamine. In the same solution, we repeat the modified electrode six times. The RSD obtained after the measurement is 2.6%, indicating that the surface of the NBC-GCE is not contaminated. In addition, Figure 8C shows the stability of the sensor. The results show that the stability of the electrode is satisfied. When stored at 4 °C for 25 days, its sensitivity remains around 95.25%.

3.7. Interference for Detecting Ractopamine. To establish the sensor selectivity, 2.0×10^{-6} M ractopamine and various interfering substances were analyzed using CV and the NBC-GCE surface (Figure 9), and the influences of

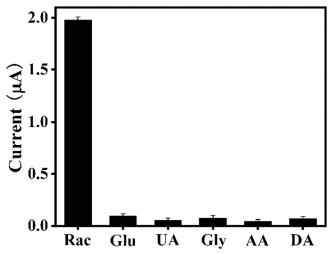

Figure 9. Influence of Glu, UA, Gly, AA, and DA on the NBC-modified GCE on the response of ractopamine.

electroactive species salbutamol (STL), brombuterol (BTL), and phenylethanolamine (PEA) on the response of ractopamine were carried out (Figure S4). It was found that at least 5 mM glucose (Glu), 1.5 mM uric acid, 1.0 mM glycine, 0.5 mM ascorbic acid, 0.2 mM dopamine, 0.5 mM salbutamol, brombuterol, and phenylethanolamine had a little bit effect on the response of 2.0×10^{-6} M ractopamine. The results show that the NBC-GCE has good selectivity in the electrochemical detection of ractopamine.

3.8. Practical Application. To confirm the practicality of our method, it was applied for ractopamine detection in pork sausages. The pork sausage sample is processed first, and then the DPV method is used for detection. Since ractopamine was not detectable in these samples, we prepared several different concentrations of standard ractopamine and added them into the sample solution. Each sample was subjected to three parallel tests, and the RSD difference was less than 5%, indicating that the results obtained by the NBC-GCE were accurate and feasible (see Table 2). It was found that the recovery rate of ractopamine was between 97.83 and 100.43%, indicating that the method could be used in practical applications.

Table 2. Ractopamine Detection in Real Samples

sample ID	μM of added Rac	detected (μM)	recovery (%)
A		0	
	1.0	0.9783	97.83
B		0	
	1.5	1.5064	100.43
C		0	
	2.0	1.9957	99.79

4. CONCLUSIONS

In summary, we adopted a green and environmentally friendly method to prepare the Nafion-biochar-Cu^{2+}/Cu^{+} material and used it for electrochemical detection of ractopamine in pork products. The obtained NBC-GCE showed great sensitivity and selectivity, low detection limit, and excellent reproducibility and stability. In addition, it has been proven that the sensor can be used in practical applications. Our work provides a novel way to treat food waste and detect ractopamine simultaneously.

■ ASSOCIATED CONTENT

Supporting Information

The Supporting Information is available free of charge at https://pubs.acs.org/doi/10.1021/acsabm.0c01314.

Study the EIS of the BC-GCE; cyclic voltammetry curves of various modified electrodes in the potassium ferricyanide solution; and relevant supplementary data of the electrode anti-interference ability test (PDF)

https://dx.doi.org/10.1021/acsabm.0c01314
ACS Appl. Bio Mater. 2021, 4, 1424−1431

AUTHOR INFORMATION

Corresponding Authors

Hetong Lin − *College of Food Science, Fujian Agriculture and Forestry University, Fuzhou 350002, Fujian, China*; Email: hetonglin@163.com

Da-Peng Yang − *College of Chemical Engineering and Materials Science, Quanzhou Normal University, Quanzhou 362000, Fujian, China; College of Food Science, Fujian Agriculture and Forestry University, Fuzhou 350002, Fujian, China*; orcid.org/0000-0003-3509-2825; Email: yangdp@qztc.edu.cn

Authors

Liping Cao − *College of Chemical Engineering and Materials Science, Quanzhou Normal University, Quanzhou 362000, Fujian, China; College of Food Science, Fujian Agriculture and Forestry University, Fuzhou 350002, Fujian, China*

Qi Ding − *College of Food Science, Fujian Agriculture and Forestry University, Fuzhou 350002, Fujian, China*

Minghuan Liu − *College of Chemical Engineering and Materials Science, Quanzhou Normal University, Quanzhou 362000, Fujian, China*

Complete contact information is available at: https://pubs.acs.org/10.1021/acsabm.0c01314

Notes

The authors declare no competing financial interest.

ACKNOWLEDGMENTS

The authors are very grateful to the Orientative Project sponsored by the Fujian Provincial Department of Science and Technology through the Grant Number 2019H0023 and to the Quanzhou City Science & Technology Program of China (Grant Number 2017G023).

REFERENCES

(1) Li, G.; Zhang, X.; Zheng, F.; Liu, J.; Wu, D. Emerging nanosensing technologies for the detection of beta-agonists. *Food Chem.* **2020**, *332*, No. 127431.

(2) Jadhav, M. R.; Pudale, A.; Raut, P.; Utture, S.; Shabeer, T. P. A.; Banerjee, K. A unified approach for high-throughput quantitative analysis of the residues of multi-class veterinary drugs and pesticides in bovine milk using LC-MS/MS and GC−MS/MS. *Food Chem.* **2019**, *272*, 292−305.

(3) Zhao, L.; Yang, S.; You, X.; He, W.; Xue, J. Novel miRNA-based biomarker panel for detection β_2-agonists in goats. *Food Chem.* **2019**, *288*, 15−21.

(4) Li, J.; Ren, X.; Diao, Y.; Chen, Y.; Wang, Q.; Jin, W.; Zhou, P.; Fan, Q.; Zhang, Y.; Liu, H. Multiclass analysis of 25 veterinary drugs in milk by ultra-high performance liquid chromatography-tandem mass spectrometry. *Food Chem.* **2018**, *257*, 259−264.

(5) Fang, X.; Chen, X.; Liu, Y.; Li, Q.; Zeng, Z.; Maiyalagan, T.; Mao, S. Nanocomposites of Zr(IV)-Based Metal−Organic Frameworks and Reduced Graphene Oxide for Electrochemically Sensing Ciprofloxacin in Water. *ACS Appl. Nano Mater.* **2019**, *2*, 2367−2376.

(6) Zeng, Z.; Fang, X.; Miao, W.; Liu, Y.; Maiyalagan, T.; Mao, S. Electrochemically Sensing of Trichloroacetic Acid with Iron(II) Phthalocyanine and Zn-Based Metal Organic Framework Nanocomposites. *ACS Sens.* **2019**, *4*, 1934−1941.

(7) Huang, Q.; Bu, T.; Zhang, W.; Yan, L.; Zhang, M.; Yang, Q.; Huang, L.; Yang, B.; Hu, N.; Suo, Y.; Wang, J.; Zhang, D. An improved clenbuterol detection by immunochromatographic assay with bacteria@Au composite as signal amplifier. *Food Chem.* **2018**, *262*, 48−55.

(8) Liu, J.; Yu, Q.; Zhao, G.; Dou, W. Ultramarine blue nanoparticles as a label for immunochromatographic on-site determination of ractopamine. *Microchim. Acta* **2020**, *187*, No. 285.

(9) Du, W.; Zhao, G.; Fu, Q.; Sun, M.; Zhou, H.; Chang, C. Combined microextraction by packed sorbent and high-performance liquid chromatography-ultraviolet detection for rapid analysis of ractopamine in porcine muscle and urine samples. *Food Chem.* **2014**, *145*, 789−795.

(10) He, L.; Su, Y.; Zeng, Z.; Liu, Y.; Huang, X. Determination of ractopamine and clenbuterol in feeds by gas chromatography−mass spectrometry. *Anim. Feed Sci. Technol.* **2007**, *132*, 316−323.

(11) Divari, S.; Berio, E.; Pregel, P.; Sereno, A.; Chiesa, L.; Pavlovic, R.; Panseri, S.; Bovee, T. F. H.; Biolatti, B.; Cannizzo, F. T. Effects and detection of Nandrosol and ractopamine administration in veal calves. *Food Chem.* **2017**, *221*, 706−713.

(12) Wang, W.; Zhang, Y.; Wang, J.; Shi, X.; Ye, J. Determination of β-agonists in pig feed, pig urine and pig liver using capillary electrophoresis with electrochemical detection. *Meat Sci.* **2010**, *85*, 302−305.

(13) Dong, B.; Zhao, S.; Li, H.; Wen, K.; Ke, Y.; Shen, J.; Zhang, S.; Shi, W.; Wang, Z. Design, synthesis and characterization of tracers and development of a fluorescence polarization immunoassay for the rapid detection of ractopamine in pork. *Food Chem.* **2019**, *271*, 9−17.

(14) Liu, Z.; Zhou, Y.; Wang, Y.; Cheng, Q.; Wu, K. Enhanced oxidation and detection of toxic ractopamine using carbon nanotube film-modified electrode. *Electrochim. Acta* **2012**, *74*, 139−144.

(15) Park, S.; Choi, K. S.; Lee, D.; Kim, D.; Lim, K. T.; Lee, K.-H.; Seonwoo, H.; Kim, J. Eggshell membrane: Review and impact on engineering. *Biosyst. Eng.* **2016**, *151*, 446−463.

(16) da Silva, R. J.; Lima, R. M. A. P.; de Oliveira, M. C. A.; Alcaraz-Espinoza, J. J.; de Melo, C. P.; de Oliveira, H. P. Supercapacitors based on (carbon nanostructure)/PEDOT/(eggshell membrane) electrodes. *J. Electroanal. Chem.* **2020**, *856*, No. 113658.

(17) Nasrollahzadeh, M.; Sajadi, S. M.; Hatamifard, A. Waste chicken eggshell as a natural valuable resource and environmentally benign support for biosynthesis of catalytically active Cu/eggshell, Fe_3O_4/eggshell and Cu/Fe_3O_4/eggshell nanocomposites. *Appl. Catal., B* **2016**, *191*, 209−227.

(18) Zhong, S. L.; Zhuang, J.; Yang, D. P.; Tang, D. Eggshell membrane-templated synthesis of 3D hierarchical porous Au networks for electrochemical nonenzymatic glucose sensor. *Biosens. Bioelectron.* **2017**, *96*, 26−32.

(19) He, X.; Yang, D.-P.; Zhang, X.; Liu, M.; Kang, Z.; Lin, C.; Jia, N.; Luque, R. Waste eggshell membrane-templated CuO-ZnO nanocomposites with enhanced adsorption, catalysis and antibacterial properties for water purification. *Chem. Eng. J.* **2019**, *369*, 621−633.

(20) Ding, Q.; Kang, Z.; He, X.; Wang, M.; Lin, M.; Lin, H.; Yang, D. P. Eggshell membrane-templated gold nanoparticles as a flexible SERS substrate for detection of thiabendazole. *Microchim. Acta* **2019**, *186*, No. 453.

(21) Zhang, D.; Zhao, H.; Fan, Z.; Li, M.; Du, P.; Liu, C.; Li, Y.; Li, H.; Cao, H. A Highly Sensitive and Selective Hydrogen Peroxide Biosensor Based on Gold Nanoparticles and Three-Dimensional Porous Carbonized Chicken Eggshell Membrane. *PLoS One* **2015**, *10*, No. e0130156.

(22) Hu, X.; Dong, S. Metal nanomaterials and carbon nanotubes-synthesis, functionalization and potential applications towards electrochemistry. *J. Mater. Chem.* **2008**, *18*, 1279.

(23) Sadanand, V.; Rajini, N.; Varada Rajulu, A.; Satyanarayana, B. Preparation of cellulose composites with in situ generated copper nanoparticles using leaf extract and their properties. *Carbohydr. Polym.* **2016**, *150*, 32−39.

(24) Lloyd, D.; Vainikka, T.; Murtomäki, L.; Kontturi, K.; Ahlberg, E. The kinetics of the Cu^{2+}/Cu^{+} redox couple in deep eutectic solvents. *Electrochim. Acta* **2011**, *56*, 4942−4948.

(25) Dou, H.; Chen, L.; Zheng, S.; Zhang, Y.; Xu, G. Q. Band structure engineering of graphitic carbon nitride via Cu^{2+}/Cu^{+} doping for enhanced visible light photoactivity. *Mater. Chem. Phys.* **2018**, *214*, 482−488.

(26) Li, Z.; Sun, Y.; Yang, Y.; Han, Y.; Wang, T.; Chen, J.; Tsang, D. C. W. Biochar-supported nanoscale zero-valent iron as an efficient catalyst for organic degradation in groundwater. *J. Hazard. Mater.* **2020**, *383*, No. 121240.
(27) Wu, W.; Li, Y.; Liu, J.; Wang, J.; He, Y.; Davey, K.; Qiao, S. Z. Molecular-Level Hybridization of Nafion with Quantum Dots for Highly Enhanced Proton Conduction. *Adv. Mater.* **2018**, *30*, No. 1707516.
(28) Bukola, S.; Liang, Y.; Korzeniewski, C.; Harris, J.; Creager, S. Selective Proton/Deuteron Transport through Nafion|Graphene| Nafion Sandwich Structures at High Current Density. *J. Am. Chem. Soc.* **2018**, *140*, 1743−1752.
(29) Yang, X.; Zhang, Y.; Hao, X.; Song, Y.; Liang, X.; Liu, F.; Liu, F.; Sun, P.; Gao, Y.; Yan, X.; Lu, G. Nafion-based amperometric H_2S sensor using Pt-Rh/C sensing electrode. *Sens. Actuators, B* **2018**, *273*, 635−641.
(30) Zhang, B.; Huang, L.; Tang, M.; Hunter, K. W.; Feng, Y.; Sun, Q.; Wang, J.; Chen, G. A nickel nanoparticle/nafion-graphene oxide modified screen-printed electrode for amperometric determination of chemical oxygen demand. *Microchim. Acta* **2018**, *185*, No. 385.
(31) Cao, L.; Kang, Z.-W.; Ding, Q.; Zhang, X.; Lin, H.; Lin, M.; Yang, D.-P. Rapid pyrolysis of Cu^{2+}-polluted eggshell membrane into a functional Cu^{2+}-Cu^{+}/biochar for ultrasensitive electrochemical detection of nitrite in water. *Sci. Total Environ.* **2020**, *723*, No. 138008.
(32) Miao, P.; Han, K.; Tang, Y.; Wang, B.; Lin, T.; Cheng, W. Recent advances in carbon nanodots: synthesis, properties and biomedical applications. *Nanoscale* **2015**, *7*, 1586−1595.
(33) Wu, J. B.; Lin, M. L.; Cong, X.; Liu, H. N.; Tan, P. H. Raman spectroscopy of graphene-based materials and its applications in related devices. *Chem. Soc. Rev.* **2018**, *47*, 1822−1873.
(34) Fu, R.; Yoshizawa, N.; Dresselhaus, M. S.; Dresselhaus, G.; Satcher, J. H.; Baumann, T. F. XPS Study of Copper-Doped Carbon Aerogels. *Langmuir* **2002**, *18*, 10100−10104.
(35) Chang, W.; Liu, S.; Qi, A.; Liu, W.; Liu, Y. In-situ synthesis of monodispersed Au nanoparticles on eggshell membrane by the extract of Lagerstroemia speciosa leaves for the catalytic reduction of 4-nitrophenol. *Mater. Res. Express* **2019**, *6*, No. 015002.
(36) Laviron, E. General expression of the linear potential sweep voltammogram in the case of diffusionless electrochemical systems. *Electroanal. Chem. Interfacial Electrochem.* **1979**, *101*, 19−28.
(37) Ma, X.; Lv, H.; Zhu, Q.; Chen, M.; Wang, Y.; Li, F. A novel sensitive electrochemical method for the detection of ractopamine in meat food via polycitrulline-modified electrode. *Food Addit. Contam., Part A* **2020**, *37*, 1459−1466.
(38) Bai, W.; Huang, H.; Li, Y.; Zhang, H.; Liang, B.; Guo, R.; Du, L.; Zhang, Z. Direct preparation of well-dispersed graphene/gold nanorod composites and their application in electrochemical sensors for determination of ractopamine. *Electrochim. Acta* **2014**, *117*, 322−328.
(39) Yang, X.; Feng, B.; Yang, P.; Ding, Y.; Chen, Y.; Fei, J. Electrochemical determination of toxic ractopamine at an ordered mesoporous carbon modified electrode. *Food Chem.* **2014**, *145*, 619−624.
(40) Wu, C.; Sun, D.; Li, Q.; Wu, K. Electrochemical sensor for toxic ractopamine and clenbuterol based on the enhancement effect of graphene oxide. *Sens. Actuators, B* **2012**, *168*, 178−184.

https://dx.doi.org/10.1021/acsabm.0c01314
ACS Appl. Bio Mater. 2021, 4, 1424−1431